



OPEN ACCESS

EDITED BY
Zizheng Guo,
Hebei University of Technology, China

REVIEWED BY
Erxing Peng,
Northwest Institute of Eco-
Environment and Resources (CAS),
China
Minghao Liu,
Chinese Academy of Sciences (CAS),
China

*CORRESPONDENCE
Zhilong Zhang,
✉ zhangzl@xju.edu.cn

SPECIALTY SECTION
This article was submitted to
Environmental Informatics and Remote
Sensing,
a section of the journal
Frontiers in Earth Science

RECEIVED 19 November 2022
ACCEPTED 12 December 2022
PUBLISHED 04 January 2023

CITATION
Liu G, Zhang Z, Cheng Z, Hao G, Hao Y
and Fu T (2023), Study on the
permeability coefficient model of
salinized frozen soil based on unfrozen
water content curve.
Front. Earth Sci. 10:1102748.
doi: 10.3389/feart.2022.1102748

COPYRIGHT
© 2023 Liu, Zhang, Cheng, Hao, Hao
and Fu. This is an open-access article
distributed under the terms of the
[Creative Commons Attribution License
\(CC BY\)](https://creativecommons.org/licenses/by/4.0/). The use, distribution or
reproduction in other forums is
permitted, provided the original
author(s) and the copyright owner(s) are
credited and that the original
publication in this journal is cited, in
accordance with accepted academic
practice. No use, distribution or
reproduction is permitted which does
not comply with these terms.

Study on the permeability coefficient model of salinized frozen soil based on unfrozen water content curve

Gunag Liu¹, Zhilong Zhang^{1*}, Zhe Cheng¹, Ge Hao¹,
Yufeng Hao² and Ting Fu²

¹College of Civil Engineering and Architecture, Xinjiang University, Ürümqi, China, ²CSCEC Xinjiang Construction & Engineering Group Co. Ltd., Ürümqi, China

Due to the fact that the permeability coefficient of salinized frozen soil is difficult to measure through experimental test, this paper develops a model of the permeability coefficient of salinized frozen soil by using SFCC curves, which takes into account the effects of velocity slip on pore wall and seepage of unfrozen water film. This model is on the basis of capillary bundle model, and combines with phase diagram theory of water-salt binary system. For the silty clay from Qinghai-Tibet Plateau and silts from Onedia, the permeability coefficient fluctuation vs. temperature is calculated using the model. The estimated calculations of the permeability coefficient model were all found to be in good agreement with the experimental data by comparison. Additionally, the variation trend of permeability coefficient of NaCl, Na₂SO₄, and Na₂CO₃ type saline soils containing different salt contents is examined. The results indicate that before saline soils freeze, NaCl does not crystallize and thus has little impact on the permeability coefficient, whereas Na₂SO₄ and Na₂CO₃ both crystallize and block the pores, the permeability coefficient decreases with decreasing temperature. Once the saline soils have frozen, the freezing temperature has a larger impact on the permeability coefficient. During the early stage of freezing, the lower the freezing temperature is, the larger the permeability coefficient is. In the late stage of freezing, the permeability coefficients with various salt contents tended to be the same.

KEYWORDS

permeability coefficient, unfrozen water content curve, velocity slip, unfrozen water film seepage, salinized frozen soil

1 Introduction

The distribution of frozen soil and saline soils in northwest and northeast China largely overlaps (Zhang et al., 2015; Wang et al., 2019), and the soils in this area are generally referred to as saline frozen soil and salinized frozen soil. Therefore, the salinized frozen soil contains the traits of saline and frozen soil soils, and the soil deformation is influenced by both salt and moisture. As a result, the infrastructure constructed in

salinized frozen soil regions is extremely vulnerable to diseases, which are primarily brought on by salt expansion and freezing. The existing study (Bing et al., 2015; Lai et al., 2021) have shown that water migration plays an important role in the freezing and thawing of frozen soil and the salt swelling and dissolution of saline soils. Further, the permeability coefficient is a key factor affecting water migration, and thus it is an important influencing factor in the study of the frost damage mechanism of infrastructure in cold regions, whether in normal frozen soil or saline frozen soil. Besides, the permeability coefficient is also a crucial component in numerous numerical models of frozen soil, including the hydrothermal coupled model (Taylor and Luthin, 1978; Zhang et al., 2021a), the hydrothermal salt coupled model (Zhang et al., 2021b; Liu et al., 2021), the hydrothermal force coupled model (Deng et al., 2021), and the hydrothermal salt force coupled model (Xu, 2021).

There have been relatively few researches conducted on the permeability coefficient of saline frozen soil, but researchers made some progress in the permeability coefficient of frozen soil. The studies are concentrated on two key points as follows: the first one is, experiments were used to directly quantify the permeability coefficient of frozen soil. In 1976, Burt and Williams (Burt and Williams, 1976) employed lactose solution for the first time to measure the head difference between two places and the flux in order to determine the permeability coefficient of frozen soil. After that, the most used method for indirectly determining the permeability coefficient of frozen soil is the seepage of antifreeze solution in the soil (Andersland et al., 1996; Tokoro et al., 2010; Watanabe and Osada, 2016). However, the experiments are difficult and the errors are large because the seepage flow is too small to be measured by weighing. The second one is, using empirical formulas to predict the permeability coefficient, and to avoid the challenges of measuring the permeability coefficient in the laboratory, empirical formulas are frequently used to predict the permeability coefficient of frozen soil. There are numerous formulas to describe the parameters of permeability coefficient, mostly including the variables saturation $k(S)$, unfrozen water content $k(\theta)$, matrix potential $k(\varphi)$, and head $k(h)$ (Richards, 1931; Averjanov, 1950; Gardner, 1958; Davidson et al., 1969). These empirical formulas are made up of curve fitting parameters and saturation permeability coefficients, but because the function expressions and parameter values vary depending on the type of soil, no empirical formula or set of fitting parameters is applicable to all soil types.

In conclusion, due to the constraints of utilizing empirical formulas, it is challenging to measure the permeability coefficients of frozen soil soils by experimental methods, and the permeability coefficients of salinized frozen soil are rarely reported. In this paper, starting from the thermodynamic theory of water film at the ice-water interface on the surface of soil particles and Gibbs-Thomson equation, a theoretical model of frozen soil permeability coefficient is proposed by using Navier-Stokes equation and Hagen-Poiseuille equation, which combines with the soil SFCC curve and based on the obtained unfrozen water film thickness of frozen pores

and the critical radius of unfrozen pores. Besides, experimental tests are used to confirm the validity of the present model. To further develop the precast ability of the proposed model, the solution phase diagram of the water-salt binary system was used to analyze the effect of salt crystallization in the soil pores prior to freezing on the permeability coefficient of frozen soil, and the permeability coefficient model of salinized frozen soil is established by modifying the permeability coefficient model of frozen soil.

In the salt freezing swelling model, the permeability coefficient is a key parameter to analyze the amount of water and salt migration and accumulation, which is conducive to accurately predict the deformation of salinized frozen soil. Therefore, it is significant to obtain the permeability coefficient change during the cooling process. The model in this article effectively combines unfrozen water, temperature, and permeability coefficient and can be used to analyze the relationship between permeability coefficient and temperature. It also provides key model parameters for the study of the salt freezing swelling model and serves as a guidance and reference for projects aimed at preventing salt freezing swelling in cold areas (Peng et al., 2021; Peng et al., 2022).

2 Model establishment of the permeability coefficient of saline frozen soil

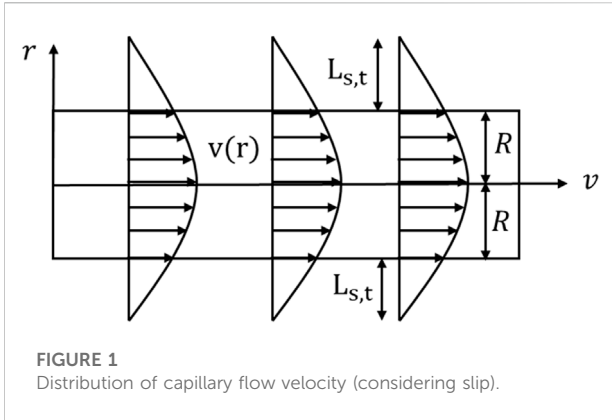
In the study of water diffusion and seepage in porous media, the capillary bundle model, a standard model to represent the internal pore structure of porous media, is crucial. The Hagen-Poiseuille equation and the Navier-Stokes equation serve as the foundation for this model. Based on the experimentally determined frozen soil SFCC curve, and considering the influence of the pore wall and unfrozen water film on water seepage in frozen soil, the permeability coefficient of saturated frozen soil is deduced as a function of initial water content and temperature.

2.1 Capillary seepage in frozen soil

The pores in soil are viewed as a network of vertical capillary tubes. The water flow in the capillary can be characterized as a laminar flow with a parabolic flow velocity distribution since the soil water percolates slowly. Without taking into account the slip of water on the pore wall, the flow velocity distribution of water passing through a capillary pore with the radius of R and length of H under pressure gradient $\Delta P = P_2 - P_1$ is

$$v(r) = \frac{1}{4\mu_{\infty}} \frac{\Delta P}{H} (R^2 - r^2) \quad (1)$$

At the radius of r , the micro ring flow of the width of dr is $dq = 2\pi r v(r)$. The Hagen-Poiseuille equation can be deduced



from the integration of the section from 0 to R in the r direction, and the sectional total flux calculated by this equation is:

$$q = \int_0^R 2\pi r v(r) dr = \frac{\pi R^4 \Delta P}{8\mu_\infty H} \quad (2)$$

where q is the total flow of water in a capillary tube of radius R; μ_∞ is the viscosity of volumetric water, which is a function of temperature (Thomas and Sansom, 1995) and can be represented as $\mu_\infty(T) = 0.6612(T - 229)^{-1.562}$.

Due to the velocity slip phenomena, as seen in Figure 1, the liquid velocity in the capillary channel close to the wall is not zero, $v(r) \neq 0$ at $r = \pm R$. Additionally, the function $\mu_\infty(T)$ is no longer usable at negative temperatures and narrow capillary tube diameters, therefore effective viscosity is used instead $\mu(d)$. When the combined water slip length $l_{s,t}$ and effective viscosity $\mu(d)$ on the pore wall are taken into account, the flow velocity distribution and water flow rate are (Holt et al., 2006)

$$v_{s,t}(r) = \frac{1}{4\mu(d)} \frac{\Delta P}{L} [(R + l_{s,t})^2 - r^2] \quad (3)$$

$$q_w = \int_{l_{s,t}}^{R+l_{s,t}} 2\pi r v_{s,t}(r) dr = \frac{\pi}{8\mu(d)} (R^4 + 4R^3 l_{s,t}) \frac{\Delta P}{L} \quad (4)$$

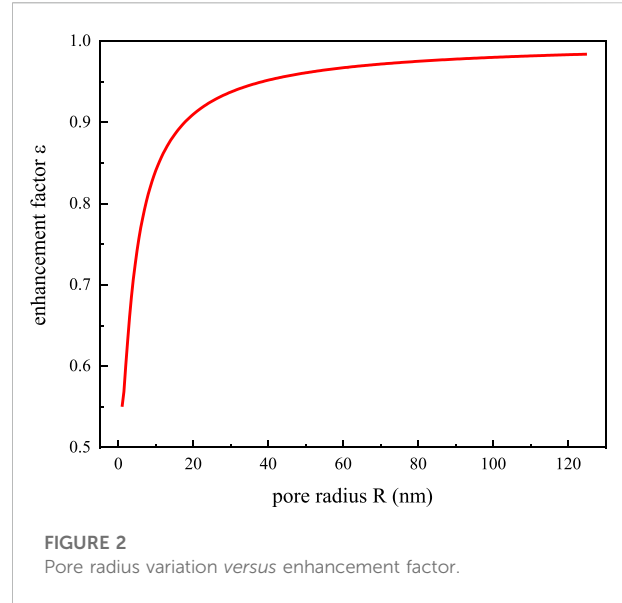
David M. Huang (Huang et al., 2008) measured the slip length of water flow wall at various contact angles, and found that the real slip length of water $l_{s,t}$ can be described as the function of soil-water contact angle as follows:

$$l_{s,t} = \frac{C}{(\cos \theta + 1)^2} \quad (5)$$

At the same time, the critical thickness can be used to compute the effective viscosity $\mu(d)$ of water in frozen soil pores, which is dependent on the area of the interface zone and the bulk water viscosity (Thomas and Mcgaughey, 2008).

$$\mu(d) = \mu_i \frac{A_i(R)}{A_t(R)} + \mu_\infty \left[1 - \frac{A_i(R)}{A_t(R)} \right] \quad (6)$$

$$A_i(R) = \pi [R^2 - (R - \lambda)^2] \quad (7)$$



where θ is the soil-water contact angle, $\theta = 25^\circ$; C is a constant, $C = .41$; μ_i is the viscosity of the fluid in the interface area, Pa · s; μ_i/μ_∞ is in a linear relationship with contact angle θ (Wu et al., 2017), $\mu_i/\mu_\infty = -0.018\theta + 3.25$; A_i is the soil-water contact area in the pore; A_t is the pore cross-sectional area; and λ is the critical thickness of the pressured fluid.

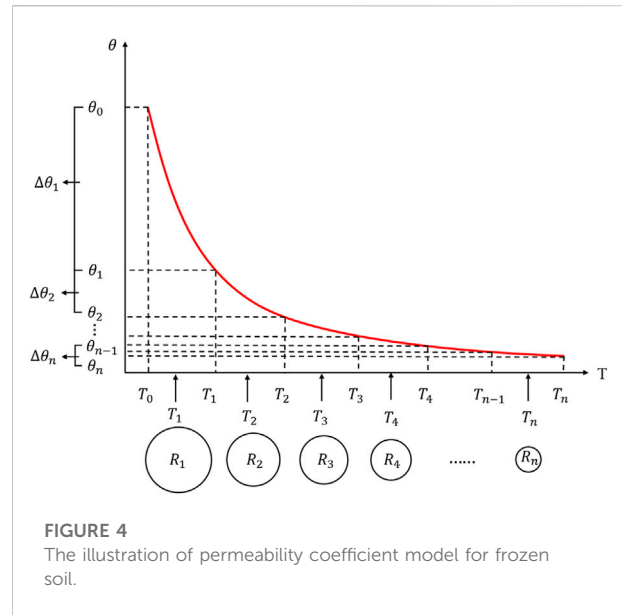
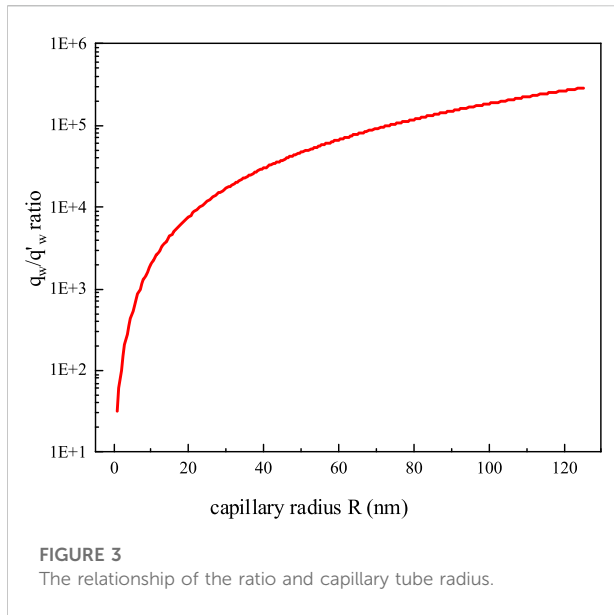
An enhancement factor is introduced, which is defined as the ratio of the measured water flux to the water flux q when no slip is considered, to examine the impact of the velocity slip phenomena on the water flux.

$$\varepsilon = \frac{q_w}{q} = \left(1 + 4 \frac{l_{s,t}}{R} \right) \frac{\mu}{\mu(d)} \quad (8)$$

As the curve shown in Figure 2, The pore radius is inversely related to the enhancement factor, and the smaller the pore, the larger the enhancement factor. When the pore radius is less than 100 nm, the trend of decreasing enhancement factor gradually accelerates, indicating that the effect of velocity slip on water flux gradually increases. Relevant researches indicate that soil pore with a radius of less than 100 nm make up more than half of all soil pores (Sasanian and Newson, 2013), thus it is crucial to account for effective water viscosity and the velocity slip phenomenon when calculating the soil seepage volume.

2.2 Filtration in unfrozen water film of frozen soil soils

The fluid in large pore in the soil freezes when the temperature drops below the freezing point, but the water near the pore wall and in the small pore doesn't freeze



because of the surface tension on pore wall (van der Waals force). On this basis, the of pores can be divided into two categories: the frozen pores and unfrozen pores. Water film seepage not only includes the capillary seepage resulting from frozen pore, but also includes the water film seepage induced by frozen pore.

At temperature T , when a capillary tube is frozen with a radius of R , the film flow velocity distribution of unfrozen water calculated by the Navier-Stokes equation yields the following results (Watanabe and Flury, 2008; Ming et al., 2022)

$$v_f(r) = \frac{\Delta P}{4\mu(d)L} \left[(R^2 - r^2) + \frac{(R^2 - r_i^2)}{\ln \frac{R}{r_i}} \ln \frac{r}{R} \right] \quad (9)$$

Besides, in the r direction, the film seepage flux of unfrozen water q'_w can be represented as the integration from r_i to R .

$$q'_w = \int_{r_i}^R 2\pi r v_f(r) dr = \frac{\Delta P \pi}{8\mu(d)L} \left[R^4 - r_i^4 - \frac{(R^2 - r_i^2)^2}{\ln \frac{R}{r_i}} \right] \quad (10)$$

The following equation can be used to determine the thickness of unfrozen water film d (Dash et al., 1995; Ishizaki et al., 1996) and the connection between temperature T and pore radius R (Mitchell et al., 2008)

$$d(T) = \left[-\frac{A}{6\pi \rho_i L_i} \left(\frac{T_i}{T_i - T} \right) \right]^{\frac{1}{3}} \quad (11)$$

$$R(T) = \frac{2\gamma_{is} \cos \theta}{\rho_i L_i} \frac{T_i}{T_i - T} \quad (12)$$

where, A is the Hamaker constant, $A = -10^{-19.5}$; ρ_i is the ice density, $\rho_i = 918 \text{Kg/m}^3$; L_i is the latent heat of ice melting, $L_i = 3.34 \times 10^5 \text{J/Kg}$; T_i is the freezing temperature of soil, in K , T is the soil temperature; γ_{is} is the ice water interface energy,

$\gamma_{is} = 4.09 \times 10^{-2} \text{J/m}^2$; and r_i is the ice nucleus radius, $r_i = R_i - d$. In order to visibly respond to the variations in magnitude of each, it is possible to calculate the ratio of water film seepage and capillary seepage.

$$\frac{q_w}{q'_w} = \frac{R^4 + 4R^3 I_{s,t}}{R^4 - r_i^4 - \frac{(R^2 - r_i^2)^2}{\ln \frac{R}{r_i}}} \quad (13)$$

A graph of the ratio of $\frac{q_w}{q'_w}$ for a capillary tube of radius R before and after freezing is depicted in Figure 3. As can be seen from the figure, as capillary diameter rises, the ratio gradually climbs to five orders of magnitude and still has a tendency to increase. This result indicates that under large tube diameter, the seepage capacity of an unfrozen water film is substantially less than the seepage capacity of unfrozen capillaries. But the seepage of unfrozen water is only 10 times as great when the tube diameter is small. Since small soil pores make up the majority of soil pores, it is important to take into account the film seepage of unfrozen water (Sasanian and Newson, 2013).

2.3 Permeability coefficient model of frozen soil

As depicted in Figure 4, the pores in soil are simplified as capillary tubes with different radiuses. Using the SFCC curve (unfrozen water content is treated as a function of temperature T), it is assumed that the temperature interval $[T_0, T_n]$ is divided into n equal parts, resulting in $T_0 > T_1 > T_2 > \dots > T_{n-1} > T_n$. Then n temperature points are obtained by taking the midpoint temperature of each temperature interval, which are $T_{01}, T_{12}, T_{23}, \dots, T_{(n-1)n}$, which represent the freezing

temperature of pores. According to Eq. 12, the pore radius corresponding to each temperature is obtained, i.e. $R_1, R_2, R_3, \dots, R_n$, and they are denoted as R_i ($i = 1, 2, 3, \dots, n$). Because unfrozen content θ is a function of temperature T , i.e., each temperature correlates to an unfrozen water content, then it is found that $\theta_0 > \theta_1 > \theta_2 > \dots > \theta_{n-1} > \theta_n$. Therefore, n temperature intervals correspond to n unfrozen water variations of $\Delta\theta_1, \Delta\theta_2, \Delta\theta_3, \dots, \Delta\theta_n$, which is denoted as $\Delta\theta_i$ ($i = 1, 2, 3, \dots, n$). In saturated soil, water fills all of the pores, and as long as the divided temperature intervals are enough, the unfrozen water variation $\Delta\theta_i$ is thought to be caused by unfrozen water crystallization in the capillary of radius R_i . Then the number n_i of capillary tubes with radius R_i can be calculated. The seepage amount of unfrozen water Q_i and the seepage amount of unfrozen water film Q'_i before and after freezing of the capillary tube with radius of R_i is obtained using Eqs. 4–10.

$$\Delta\theta_i = \pi \sum_{i=1}^n n_i R_i^2 \quad (14)$$

$$Q_i = \frac{n_i \pi}{8\mu(d)} (R_i^4 + 4R_i^3 l_{st}) \frac{\Delta P}{H} \quad (15)$$

$$Q'_i = \frac{n_i \pi}{8\mu(d)} \left[R^4 - r_i^4 - \frac{(R^2 - r_i^2)^2}{\ln \frac{R}{r_i}} \right] \frac{\Delta P}{H} \quad (16)$$

At the meantime, the water migration path is idealized to occur in a curving capillary. Assuming that the frozen soil has a length of L and a height of H ($H < L$), and combining Eqs. 15, 16, the water flux of frozen soil can be described as:

$$Q_w = \frac{\rho_w g \pi}{8\mu(d)} \left(\sum_{i=j+1}^n (R_i^4 + 4R_i^3 l_i) + \sum_{i=1}^j \frac{n_i}{\xi_i} \left[R^4 - r_i^4 - \frac{(R^2 - r_i^2)^2}{\ln \frac{R}{r_i}} \right] \right) \quad (17)$$

where: $j=0, 1, 2, \dots, n-1$, and the corresponding j rises by one for each temperature interval of temperature decrease; ξ is the ratio of the soil column length H to the actual path of water seepage L ($\xi = L/H$), $\xi_i = 1 + 0.41 \ln(1/\theta_i)$ (Xiao et al., 2015); $\Delta P = \rho_w g H$; n is the total type number of pore radius in unit area; n_i is the number of pores with the radius of R_i in unit area.

Assuming that water seepage in frozen soil follows Darcy's law, Eq. 17 can be combined to determine the permeability coefficient of frozen soil per unit area.

$$K = \frac{\rho_w g \pi}{8A\mu(d)} \left(\sum_{i=j+1}^n (R_i^4 + 4R_i^3 l_i) + \sum_{i=1}^j \frac{n_i}{\xi_i} \left[R^4 - r_i^4 - \frac{(R^2 - r_i^2)^2}{\ln \frac{R}{r_i}} \right] \right) \quad (18)$$

According to Eq. 18, when $j=0$, K is the permeability coefficient of the melted soil under the same conditions. The water in the melted soil primarily flows in large pores, and the pore walls almost have no effect on water flow which can be disregarded. The permeability coefficient of melted soil can then be written as:

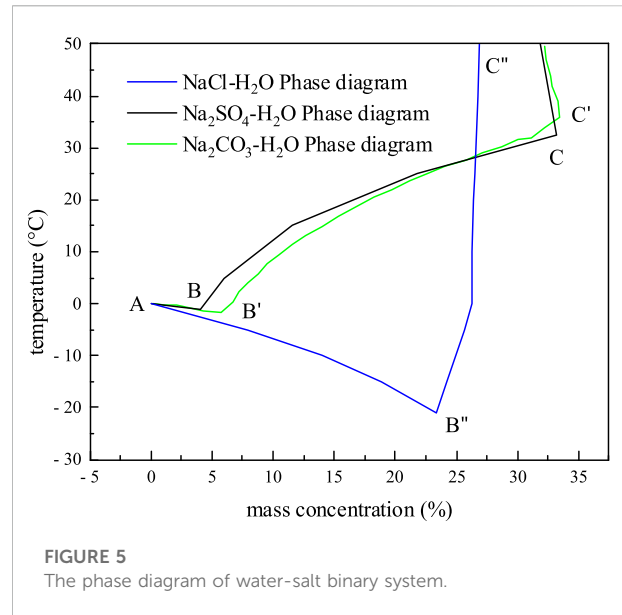


FIGURE 5 The phase diagram of water-salt binary system.

$$K_0 = \frac{\rho_w g \pi}{8A\mu_\infty} \sum_{i=1}^n \frac{n_i}{\xi_i} R_i^4 \quad (19)$$

Consequently, the frozen soil permeability coefficient can also be expressed as:

$$K = \frac{K'_0 \mu_\infty}{\mu(d)} \left(\sum_{i=j+1}^n (R_i^4 + 4R_i^3 l_i) + \sum_{i=1}^j \frac{n_i}{\xi_i} \left[R^4 - r_i^4 - \frac{(R^2 - r_i^2)^2}{\ln \frac{R}{r_i}} \right] \right) \times \frac{1}{\sum_{i=1}^n \frac{n_i}{\xi_i} R_i^4} \quad (20)$$

K'_0 is the measured value of permeability coefficient of melted soil.

2.4 Permeability coefficient model of saline soils

It is required to examine the impact of the amount of salt crystallization on the permeability coefficient in order to adapt the permeability coefficient model of frozen soil to saline frozen soil. The freezing temperature curve of ice, AB, which is the precipitation ice line, and the solubility curve of salt, BC, which is the precipitation salt line, intersect at the eutectic point B, as the phase diagram of the water-salt binary system with three salts, Na_2CO_3 , Na_2SO_4 , and NaCl shown in Figure 5. The precipitation ice line, precipitation salt line, and eutectic point separate the solution phase diagram into four areas, i.e. the unsaturated salt solution, ice-salt solution, ice-crystalline salt, and crystalline salt-salt solution. The phase diagram can be used to predict the direction of several changes that will take place in the system

TABLE 1 Physicochemical characteristics of crystalline salts.

Solution type	Crystalline salt molecular formula	Molecular weight	Specific gravity	Eutectic temperature	Eutectic concentration (%)
Sodium sulfate	Na ₂ SO ₄ · 10H ₂ O	322.22	1.48	-1.2	4
Sodium carbonate	Na ₂ CO ₃ · 10H ₂ O	286.16	1.46	-1.8	5.8
Sodium Chloride	NaCl · 2H ₂ O	76.44	1.52	-21.1	23.3

during the temperature lowering process. It is possible to determine the order of phase change, freezing temperature, eutectic temperature, eutectic concentration, and other important parameters of saline soils during the process of temperature reduction and further analyze the amount of salt crystallization. In Table 1, the values of specific parameters during the crystallization of various salt solutions are given.

Through electron microscopy, Jing Zhao (Zhao and Luo, 2019) discovered that the salt solution in the pores gradually increases in salt crystallization as the temperature decreases. These salt crystals adsorb around the pores, and gradually reduce the pore size. As a result, the permeability coefficient model of impregnated frozen soil only needs to be modified the R_i in the permeability coefficient model of frozen soil.

If it is assumed that the salt solution is contained in a capillary tube with a radius of R_i ($i = 1 \dots n$), the solution is always saturated after the salt precipitation. If the supersaturation of solution is not taken into account, the following equation is obtained:

$$C' = \begin{cases} n(T) & C > n(T) \\ C & C \leq n(T) \end{cases} \quad (21)$$

where, C is the initial mass concentration of solution, C' is the subsequent mass concentration of solution after cooling, R_i is the initial pore radius, R_i' is the subsequent pore radius after the salt precipitation due to cooling, and $n(T)$ is the solubility curve.

Assuming that the salt crystals are evenly deposited on the pore walls after salt precipitation, the quantity of salt crystallization equals the amount of variation in the pore:

$$\frac{M_c}{M\rho_c} \left(\pi R_i'^2 \frac{C}{100 - C} - \pi R_i^2 \frac{C'}{100 - C'} \right) = \pi R_i^2 - \pi R_i'^2 \quad (22)$$

M_c where M_c is the molecular weight of salt after crystallization, M is the molecular weight of salt, and ρ_c is the specific gravity of the crystalline salt. For the same salt $\frac{M_c}{M\rho_c}$ is a constant value and let $\frac{M_c}{M\rho_c} = \alpha$, then Eq. 23 can be used to determine the pore radius R_i' after salt precipitation:

$$R_i' = R_i \sqrt{\frac{[\alpha C - (100 - C)](100 - C')}{[\alpha C' - (100 - C')](100 - C)}} \quad (23)$$

Once the temperature is lowered to the eutectic temperature, the pore solution in soil mass gradually freezes. Since the

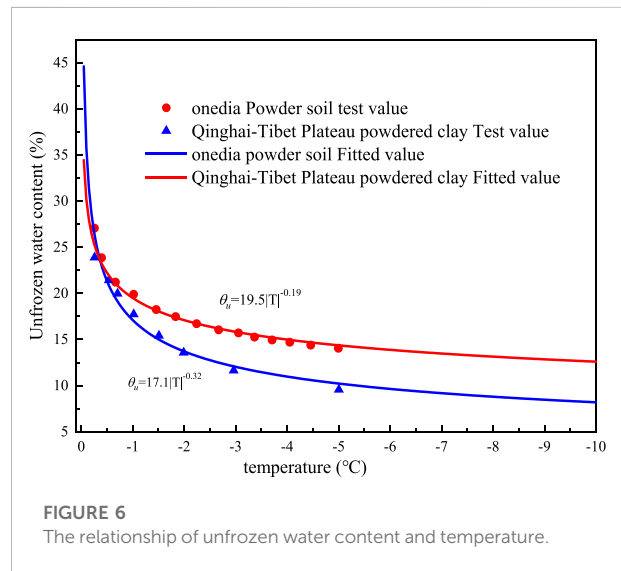


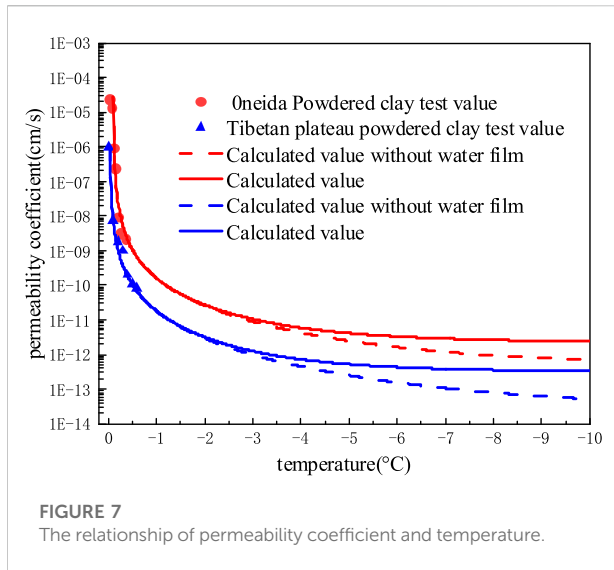
FIGURE 6 The relationship of unfrozen water content and temperature.

solubility of salt does not significantly change, the concentration of the salt solution in the pore after the soil freezes is regarded as the eutectic concentration. Eq. 24 can be used to obtain the freezing temperature T_i' for a pore with the size of R_i' considering the impact of salt (Scherer, 1999):

$$T_i' = \frac{T_0}{1 - \frac{T_0 R^*}{L_i} \ln a_w} - \frac{\sigma_{ls}}{\rho_i L_i} \frac{T_i}{R_i} \quad (24)$$

a_w where, a_w is the water activity, which is used to solve the freezing temperature T_i of salt solution, and the water activity can be calculated using the Pitzer model, R^* is the universal gas constant, and T_0 is the freezing temperature of pure water.

In conclusion, in this permeability coefficient model of salinized frozen soil, only the SFCC curve of frozen soil and the permeability coefficient of frozen soil need to be precise measured under the same conditions as well as the phase diagram of salt solution. Then the variation relationship between the permeability coefficient of frozen soil and temperature can be theoretically analyzed, as well as the variation relationship between the permeability coefficient of salinized soil.



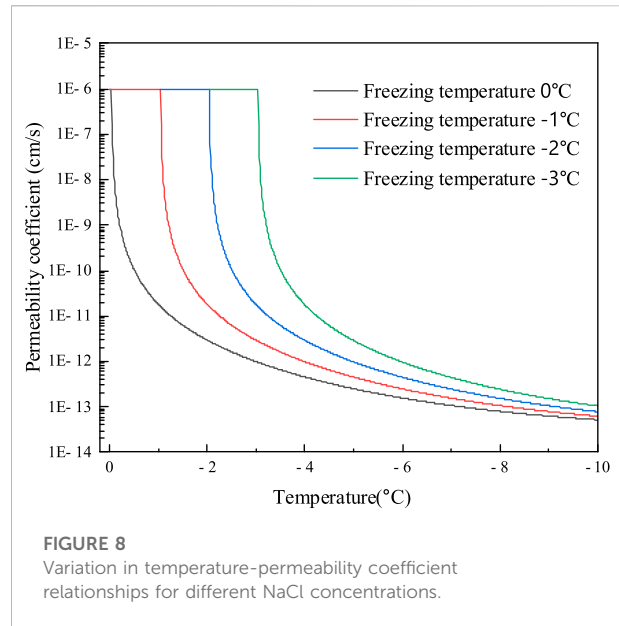
3 Calculation of permeability coefficient model

3.1 Verification of permeability coefficient model of frozen soil

As seen in Figure 6, the unfrozen water content of the silty clays from the Tibetan plateau and the silt from Oneida fluctuates with temperature (Burt and Williams, 1976; Hu et al., 2016), and the initial volumetric water contents of the two soils are 50% and 48%, respectively. The unfrozen water content decreases with decreasing temperature, and there is a general power function relationship between the two parameters. The measured temperature of data points ranges from 0 to -5°C . In order to improve prediction capacity of the proposed model, the whole SFCC curve can be derived for by fitting the functional relationship between the above two parameters.

As depicted in Figure 7, at the temperatures above -2°C , the difference between the calculated results from the model that takes the influence of an unfrozen water film into account and that does not is relatively minimal. In both cases, the predicted values of the proposed model essentially follow the trend of the test results of soil. When the temperature drops to -5°C , there is a discrepancy between the calculated results of the two models of around one time, and when the temperature drops to -10°C , there is a difference of about nine times. The primary explanation is that, when considering the seepage of unfrozen water film, as temperature decreases, pore water gradually freezes. As a result, the seepage of unfrozen water film eventually occupies the leading position of frozen soil water seepage.

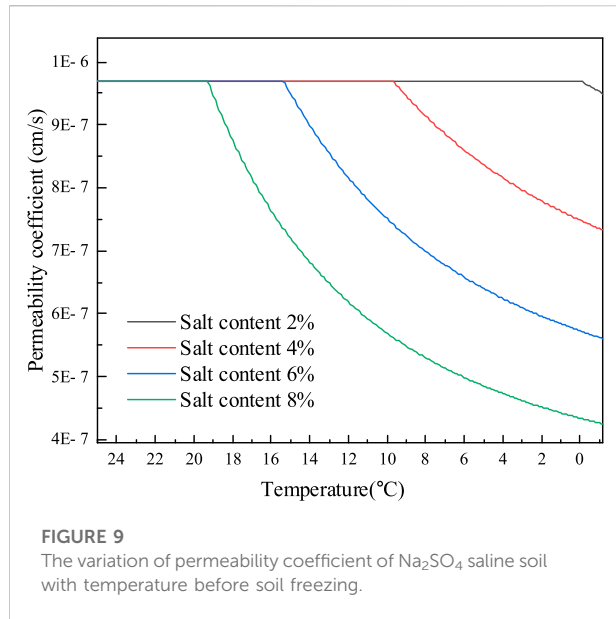
The relevant research (Burt and Williams, 1976; Chen and Zhang, 2020) shows that when the temperature is higher than -2°C , the soil still contains a lot of unfrozen water, the



soil permeability coefficient is large, and the water salinity still has a certain seepage capacity; When the temperature is lower than -2°C , the content of unfrozen water is greatly reduced, the permeability coefficient of soil is small, and the water salinity almost does not percolate. Therefore, the influence of unfrozen water film seepage is ignored in the calculation of permeability coefficient model of saline frozen soil. In the salt frost heaving model, when the temperature is lower than -2°C , the calculated result of the model considering the seepage permeability coefficient of unfrozen water film is larger, so the calculated salt frost heaving deformation is larger. This may be conducive to accurate analysis of frost heave deformation of salinized salt.

3.2 Permeability coefficient of NaCl saline soil

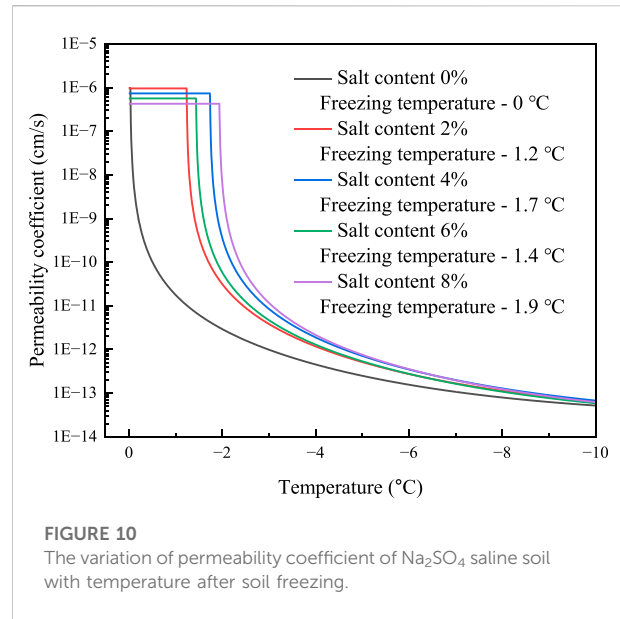
As noted in Table 1, the eutectic temperature of NaCl solution is -21.1°C , and the eutectic concentration is 23.3%, which is substantially higher than the solution concentration in the pores of saline soils. As a result, in the process of temperature decrease, water freezing takes place in the soil before NaCl crystallizes, and NaCl primarily influences the initial freezing point of soil. According to the NaCl phase diagram, the solutions with freezing temperatures of 0, -1 , -2 , -2 , and -3°C are prepared and added into the samples of powdered clay from the Qinghai-Tibet Plateau with the mass concentrations of 1.86%, 3.59%, 5.20%, and 6.64%, respectively, and the salt contents of the prepared soil samples are .59%, 1.16%, 1.71%, and 2.22%, respectively. The calculation results of the permeability coefficient model of NaCl-saline soil is depicted in Figure 8. It is shown that the permeability coefficient gradually



lowers as the temperature steadily drops and eventually tends to stabilize. The change in permeability coefficient exhibits a tendency of steep first and then slow change when the soil pores freeze in order from large to small. In terms of numerical magnitude, the initial freezing temperature steadily drops as NaCl content rises, and at the same temperature, the permeability coefficient increases as the amount of unfrozen water increases.

3.3 Permeability coefficient of Na₂SO₄ saline soil

Since Na₂SO₄ will precipitate before the soil freezes and thus has a less substantial impact on the freezing temperature of the soil than NaCl. Table 1 demonstrates that the eutectic temperature of Na₂SO₄ solution is -1.2°C and the eutectic concentration is 4%. The Na₂SO₄ solutions comprising 2%, 4%, 6%, and 8% salt were fabricated, and the mass concentrations of the pore solutions of the powdered clay samples from the Qinghai-Tibet Plateau are 6.01%, 11.34%, 16.11%, and 20.38%, respectively. Due to the presence of supersaturation of the pore solution concentration after freezing, it is difficult to calculate the first freezing temperature using the Pitzer theory. Thus, the initial freezing temperature of the soil will be determined using existing studies (Wan et al., 2015; Xiao et al., 2018). Before the soil freezes, salt will precipitate from the Na₂SO₄ solution during the dropping process of temperature, causing the permeability coefficient to start to fall. This is shown in Figure 9 and Figure 10 for the computation of the permeability coefficient model for sodium sulfate-saline soils. The beginning temperature for salt



precipitation increases along with the Na₂SO₄ content, as does the volume of precipitated mannite. The permeability coefficient of the soil with an 8% salt concentration steadily drops to 4.25×10^{-7} at 19.2°C, which was 56% lower than the permeability coefficient of the soil without salt. After soil freezes, the permeability coefficient changes as the temperature progressively drops, and the change is initially steep, then becomes gently, while eventually converges. The permeability coefficient is relatively high, and the initial freezing temperature directly affects it because the amount of unfrozen water steadily increases as the starting freezing temperature decreases.

3.4 Permeability coefficient of Na₂CO₃ saline soil

Na₂CO₃ will crystallize and precipitate before the soil freezes, as indicated in Table 1, where the eutectic temperature of the solution is -1.8°C and the eutectic concentration is 5.8%. The permeability coefficient of Na₂CO₃ saline soils is calculated using the method for Na₂SO₄ saline soils due to the similarity between these two solutions. The initial freezing temperature of the soils is determined from experiment (Hui and Wei, 2011). The powdered clay soils of the Tibetan plateau, with mass concentrations of 6.01%, 11.34%, 16.11%, and 20.38% are manufactured, and pore solutions are prepared using salt concentrations of 2%, 4%, 6%, and 8%. The calculation results of the permeability coefficient of sodium carbonate saline soils are given in Figures 11, 12. The findings show that the soils with 2% salt content do not crystallize before freezing and that the permeability coefficient remains constant. During the decreasing process of temperature, salt gradually precipitates in the pores of

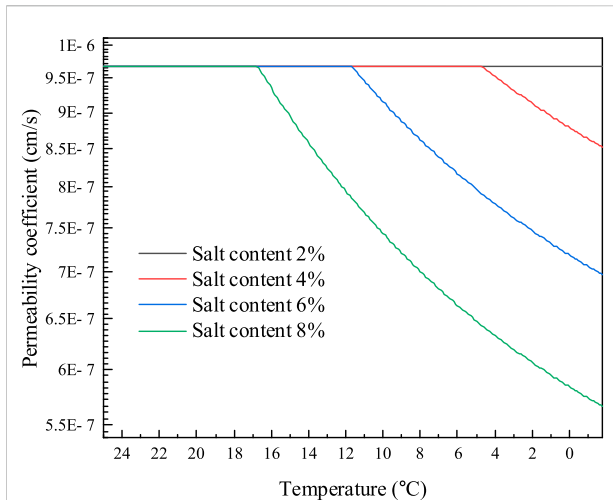


FIGURE 11
The variation of permeability coefficient of Na_2CO_3 saline soil and temperature before soil freezing.

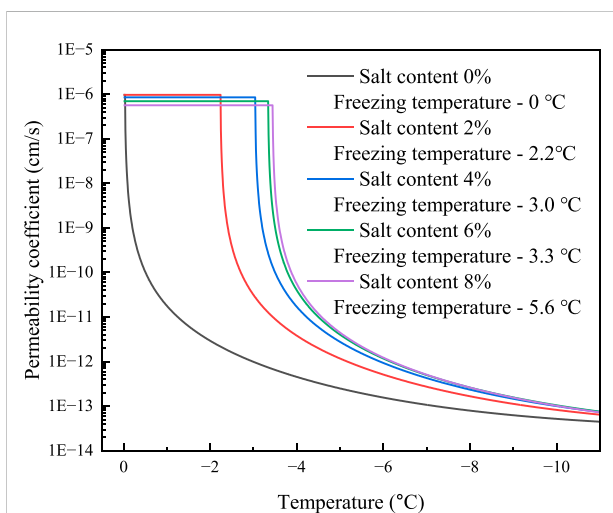


FIGURE 12
The variation of permeability coefficient of Na_2CO_3 saline soil and temperature after soil freezing.

soil with salt contents of 2%, 4%, and 6%, and the permeability coefficient of the soil gradually declines. Likewise, the higher the soil's salt content, the higher the temperature at which the salt begins to precipitate out, and the lower the permeability coefficient at the same temperature. The permeability coefficient of soil with an 8% salt content drops by around 41%, from 9.68×10^{-7} cm/s to 5.66×10^{-7} cm/s. When the soil freezes, the permeability coefficient is comparatively larger under the same temperature conditions and the amount of unfrozen water increases due to the higher Na_2CO_3 content and lower initial freezing temperature.

4 Discussion

On the basis of the thermodynamic theory of water film (Dash et al., 1995) and Gibbs-Thomson equation (Mitchell et al., 2008), the soil pores are simplified to capillary tubes, and the Navier-Stokes equation and Hagen-Poiseuille equation are combined with experimental data to obtain SFCC. Then, a model of the permeability coefficient of frozen soil that takes into account the effect of film seepage of unfrozen water is established, which was compared with the experimental results and shows a good reliability. At the same time, there are many areas that need further study.

- 1) In order to fill the gap in the theoretical analysis of the permeability coefficient of saline soil, the permeability coefficient model of saline frozen soil was developed on the basis of the frozen soil permeability coefficient model. This model considers the effects of sodium chloride, sodium sulfate, and sodium carbonate contents on freezing temperature as well as the effects of salt crystallization blocking pore space using the phase diagram theory of water-salt binary system. It is difficult to measure the permeability coefficient of salinized frozen soil soils and there are few related studies. The existing studies only measured the permeability coefficients of different salt contents under positive temperature conditions (Deng et al., 2006) and unfrozen water content curves (Ma et al., 2016). This paper also only theoretically analyzes the trend of permeability coefficients in saline soils during temperature reduction, so the credibility of the model results needs to be further confirmed by experiments.
- 2) There is a certain error between the permeability coefficient at the initial stage of freezing and the measured permeability coefficient. The reason may be that the power function form is used to fit the SFCC curve (Anderson and Tice, 1972; Chai et al., 2018), which tends to be infinite near 0°C , and it cannot accurately reflect the unfrozen water content, so there is a certain error. Therefore, the model should be modified by measuring the permeability coefficient of the melted soil.
- 3) The adsorption and desorption of particle components to soil particles are related to several factors such as temperature, soil structure, particle type, etc. (Bai et al., 2021; Bai et al., 2022) Considering the complexity of particle adsorption and desorption, this paper does not consider particle adsorption and desorption in analyzing the percolation of salt solution in soil during temperature reduction. The theory of particle adsorption and desorption can be combined with the theory of permeability coefficient in this paper, which may have some application prospects in the analysis of soil pollutant diffusion. At the same time, after the salt solution is added to the soil, the particles adsorb on the surface of soil particles, and the pore solution concentration is bound to decrease, which has a certain influence on the

freezing temperature of the soil and the amount of salt crystallization, and considering this issue will make the permeability coefficient model of salinized frozen soil more reasonable.

- 4) In the present day machine learning methods are heavily applied to the assessment of slope stability (Chang et al., 2020; Huang et al., 2020c), the permeability coefficient as one of the important parameters of the soil is greatly associated with the slope landslide (Jian et al., 2016; Hongwei and Fan, 2021), and the freezing process of the frozen soil is regarded as the drying process of the soil (Spaans and Baker, 1996), and the permeability coefficient of the soil under different water contents can be analyzed by this model, which will be beneficial to the accuracy of the machine learning model in assessing the stability of the slope (Huang et al., 2020a; Huang et al., 2020b). At the same time, the permeability coefficient is an important parameter in the multi physical field coupling model of soil mass, which has certain advantages in analyzing the mechanical properties and deformation of soil mass in the process of underground mineral mining (Li et al., 2022; Tang et al., 2023). In other porous media, the method of this model can be used to analyze the permeability coefficients of different porous materials and different pore solution contents, which has a broad application prospect.

5 Conclusion

- 1) By comparing the calculation results of the model with and without considering the unfrozen water film, it is found that: When the temperature drops to -5°C , there is a discrepancy between the calculated results of the two models of around one time, and when the temperature drops to -10°C , there is a difference of about nine times. Since the permeability coefficient of soil mass is too small after the temperature is reduced to -2°C , it is not significant to consider the permeability of unfrozen water film.
- 2) Before the soil freezes, the type of salt is the primary factor impacting the permeability coefficient. In this condition, NaCl does not crystallize and has no influence on the permeability coefficient. For sodium sulfate and sodium carbonate, which are crystallizable salts with similar properties, when the salt content is high, the salt will crystallize when the soil is not frozen, and the permeability coefficient of the soil with salt crystallization starts to decrease. The higher the salt content, the faster the decreasing rate.
- 3) After the soil freezes, the permeability coefficient is directly impacted by the freezing temperature. the lower the beginning freezing temperature, the larger the permeability coefficient. Because different types of saline soil have different

influences on freezing temperature, the reason may be that the easily crystallized salt precipitates a large amount of salt before the soil freezes. in general, the permeability coefficient of saline soils after freezing is not directly related to the salt concentration.

Data availability statement

The original contributions presented in the study are included in the article/supplementary material, further inquiries can be directed to the corresponding author.

Author contributions

GL's main task is to collate data and write articles. ZZ is the data provider, fund acquirer and innovation point proposer of this article. ZC mainly provided many valuable suggestions for this article. GH, YH, and TF provided help in the article modification.

Funding

Natural Science Foundation of Xinjiang Uygur Autonomous Region: Research on the Mechanism and Effect of High Temperature Frozen Soil Solidification (2020D01C025), 2020.01-2022.12. The research described in this paper was financially supported by 2020D01C025.

Conflict of interest

The authors YH and TF were employed by CSCEC Xinjiang Construction & Engineering Group Co. Ltd.

The remaining authors declare that the research was conducted in the absence of any commercial or financial relationships that could be construed as a potential conflict of interest.

Publisher's note

All claims expressed in this article are solely those of the authors and do not necessarily represent those of their affiliated organizations, or those of the publisher, the editors and the reviewers. Any product that may be evaluated in this article, or claim that may be made by its manufacturer, is not guaranteed or endorsed by the publisher.

References

- Andersland, O. B., Wiggert, D. C., and Davies, S. H. (1996). Hydraulic conductivity of frozen granular soils. *J. Environ. Eng.* 122, 212–216. doi:10.1061/(asce)0733-9372(1996)122:3(212)
- Anderson, D. M., and Tice, A. R. (1972). Predicting unfrozen water contents in frozen soils from surface area measurements. *Highw. Res. Rec.* 10, 105. doi:10.1016/0022-4898(73)90017-7
- Averjanov, S. F. (1950). About permeability of subsurface soils in case of incomplete saturation. *Engl. Collect.* 7, 19–21.
- Bai, B., Bai, F., Li, X., Nie, Q., Jia, X., and Wu, H. (2022). The remediation efficiency of heavy metal pollutants in water by industrial red mud particle waste. *Environ. Technol. Innovation* 28, 102944. doi:10.1016/j.eti.2022.102944
- Bai, B., Nie, Q., Zhang, Y., Wang, X., and Hu, W. (2021). Cotransport of heavy metals and SiO₂ particles at different temperatures by seepage. *J. Hydrology* 597, 125771. doi:10.1016/j.jhydrol.2020.125771
- Bing, H., He, P., and Zhang, Y. (2015). Cyclic freeze-thaw as a mechanism for water and salt migration in soil. *Environ. Earth Sci.* 74, 675–681. doi:10.1007/s12665-015-4072-9
- Burt, T. P., and Williams, P. J. (1976). Hydraulic conductivity in frozen soils. *Earth Surf. Process.* 1, 349–360. doi:10.1002/esp.3290010404
- Chai, M., Zhang, J., Zhang, H., Mu, Y., Sun, G., and Yin, Z. (2018). A method for calculating unfrozen water content of silty clay with consideration of freezing point. *Appl. Clay Sci.* 161, 474–481. doi:10.1016/j.clay.2018.05.015
- Chang, Z., Du, Z., Zhang, F., Huang, F., Chen, J., Li, W., et al. (2020). Landslide susceptibility prediction based on Remote sensing images and GIS: Comparisons of supervised and unsupervised machine learning models. *Remote Sens.* 12, 502. doi:10.3390/rs12030502
- Chen, L., and Zhang, X. (2020). A model for predicting the hydraulic conductivity of warm saturated frozen soil. *Build. Environ.* 179, 106939. doi:10.1016/j.buildenv.2020.106939
- Dash, J. G., Fu, H., and Wettlaufer, J. S. (1995). The premelting of ice and its environmental consequences. *Rep. Prog. Phys.* 58, 115–167. doi:10.1088/0034-4885/58/1/003
- Davidson, J. M., Stone, L. R., Nielsen, D. R., and Larue, M. E. (1969). Field measurement and use of soil-water properties. *Water Resour. Res.* 5, 1312–1321. doi:10.1029/WR005i006p01312
- Deng, Q., Liu, X., Zeng, C., He, X., Chen, F., and Zhang, S. (2021). A freezing-thawing damage characterization method for highway subgrade in seasonally frozen regions based on thermal-hydraulic-mechanical coupling model. *Sensors* 21 (18), 6251. doi:10.3390/s21186251
- Deng, Y., He, P., Zhou, C., Li, Y., Fang, J., Huang, S., et al. (2006). Experimental study of permeability coefficient of saline soils. *J. Glaciol. Geocryol.* 28, 772–775.
- Gardner, R. W. (1958). Some steady-state solutions of the unsaturated moisture flow equation with application to evaporation from a water table. *Soil Sci.* 85, 228–232. doi:10.1097/00010694-195804000-00006
- Holt, J. K., Park, H. G., Wang, Y., Stadermann, M., Artyukhin, A. B., Grigoropoulos, C. P., et al. (2006). Fast mass transport through sub-2-nanometer carbon nanotubes. *Science* 312, 1034–1037. doi:10.1126/science.1126298
- Hongwei, W., and Fan, Z. (2021). Influence of saturated permeability coefficient variation on failure probability of slope. *J. South China Univ. Technol. Nat. Sci. Ed.* 49, 95–102.
- Hu, Z., Jianming, Z., Zhilong, Z., and Mingtang, C. (2016). Measurement of hydraulic conductivity of Qinghai-Tibet Plateau silty clay under subfreezing temperatures. *Chin. J. Geotechnical Eng.* 38, 1030–1035. doi:10.11779/CJGE201606008
- Huang, D. M., Sendner, C., Horinek, D., Netz, R. R., and Bocquet, L. (2008). Water slippage versus contact angle: A quasiuniversal relationship. *Phys. Rev. Lett.* 101, 226101. doi:10.1103/PhysRevLett.101.226101
- Huang, F., Cao, Z., Guo, J., Jiang, S.-H., Li, S., and Guo, Z. (2020a). Comparisons of heuristic, general statistical and machine learning models for landslide susceptibility prediction and mapping. *Catena* 191, 104580. doi:10.1016/j.catena.2020.104580
- Huang, F., Cao, Z., Jiang, S.-H., Zhou, C., Huang, J., and Guo, Z. (2020b). Landslide susceptibility prediction based on a semi-supervised multiple-layer perceptron model. *Landslides* 17, 2919–2930. doi:10.1007/s10346-020-01473-9
- Huang, F., Zhang, J., Zhou, C., Wang, Y., Huang, J., and Zhu, L. (2020c). A deep learning algorithm using a fully connected sparse autoencoder neural network for landslide susceptibility prediction. *Landslides* 17, 217–229. doi:10.1007/s10346-019-01274-9
- Hui, B., and Wei, M. (2011). Experimental study on freezing point of saline soil. *J. Glaciol. Geocryol.* 33, 1106–1113.
- Ishizaki, T., Maruyama, M., Furukawa, Y., and Dash, J. G. (1996). Premelting of ice in porous silica glass. *J. Cryst. Growth* 163, 455–460. doi:10.1016/0022-0248(95)00990-6
- Jian, L., Chen, Z., and Huang, J. (2016). Effects of spatial variability of saturated permeability on slope stability. *Eng. J. Wuhan Univ.* 49, 831–837.
- Lai, Y. M., You, Z. M., and Zhang, J. (2021). Constitutive models and salt migration mechanisms of saline frozen soil and the-state-of-the-practice countermeasures in cold regions. *Cold Regions Sci. Technol.* 13, 1–17. doi:10.3724/SP.J.1226.2021.00001
- Li, X., Wang, Y., Hu, Y., Zhou, C., and Zhang, H. (2022). Numerical investigation on stratum and surface deformation in underground phosphorite mining under different mining methods. *Front. Earth Sci.* 10, 831856. doi:10.3389/feart.2022.831856
- Liu, J., Yang, P., and Yang, Z. (2021). Water and salt migration mechanisms of saturated chloride clay during freeze-thaw in an open system. *Cold Reg. Sci. Tech.* 186, 103277. doi:10.1016/j.coldregions.2021.103277
- Ma, M., Hui, B., and Li, G. (2016). Experimental research on unfrozen water content of sodium sulphate saline soil. *J. Glaciol. Geocryol.* 38, 963–969. doi:10.7522/j.issn.1000-0240.2016.0110
- Ming, F., Pei, W., Zhang, M., and Chen, L. (2022). A hydraulic conductivity model of frozen soils with the consideration of water films. *Eur. J. Soil Sci.* 73, e13210. doi:10.1111/ejss.13210
- Mitchell, J., Webber, J. B. W., and Strange, J. H. (2008). Nuclear magnetic resonance cryoporometry. *Phys. Rep.* 461, 1–36. doi:10.1016/j.physrep.2008.02.001
- Peng, E.-X., Hu, X.-Y., Sheng, Y., Wu, J.-C., Cao, W., Yang, Q.-F., et al. (2022). Thermal effect of the accumulated water with different depths on permafrost subgrade in cold regions. *Adv. Clim. Change Res.* S1674927822000855. doi:10.1016/j.accre.2022.08.003
- Peng, E.-X., Sheng, Y., Hu, X.-Y., Wu, J.-C., and Cao, W. (2021). Thermal effect of thermokarst lake on the permafrost under embankment. *Adv. Clim. Change Res.* 12, 76–82. doi:10.1016/j.accre.2020.10.002
- Richards, A. L. (1931). Capillary conduction of liquids through porous mediums. *Physics* 1, 318–333. doi:10.1063/1.1745010
- Sasanian, S., and Newson, T. A. (2013). Use of mercury intrusion porosimetry for microstructural investigation of reconstituted clays at high water contents. *Eng. Geol.* 158, 15–22. doi:10.1016/j.enggeo.2013.03.002
- Scherer, G. W. (1999). Crystallization in pores. *Cem. Concr. Res.* 29, 1347–1358. doi:10.1016/S0008-8846(99)00002-2
- Spaans, E. J. A., and Baker, J. M. (1996). The soil freezing characteristic: Its measurement and similarity to the soil moisture characteristic. *Soil Sci. Soc. Am. J.* 60, 13–19. doi:10.2136/sssaj1996.03615995006000010005x
- Tang, Q., Chen, Y., Jia, R., Guo, W., Chen, W., Li, X., et al. (2023). Effect of clay type and content on the mechanical properties of clayey silt hydrate sediments. *J. Petroleum Sci. Eng.* 220, 111203. doi:10.1016/j.petrol.2022.111203
- Taylor, G. S., and Luthin, J. N. (1978). A model for coupled heat and moisture transfer during soil freezing. *Rev. Can. De Géotechnique* 15, 548–555. doi:10.1139/t78-058
- Thomas, H. R., and Sansom, M. R. (1995). Fully coupled analysis of heat, moisture, and air transfer in unsaturated soil. *J. Eng. Mech.* 121, 392–405. doi:10.1061/(asce)0733-9399(1995)121:3(392)
- Thomas, J. A., and Mcgaughey, A. (2008). Reassessing fast water transport through carbon nanotubes. *Nano Lett.* 8, 2788–2793. doi:10.1021/nl8013617
- Tokoro, T., Ishikawa, T., and Akagawa, S. (2010). A method for permeability measurement of frozen soil using an ice lens inhibition technique. *Jiban Kogaku Janaru* 5, 603–613. doi:10.3208/jgs.5.603
- Wan, X., Lai, Y., and Wang, C. (2015). Experimental study on the freezing temperatures of saline silty soils: Study on the freezing temperatures of sulfate saline silty soils. *Permafrost. Periglacial Process.* 26, 175–187. doi:10.1002/ppp.1837
- Wang, X., Chen, R., Liu, G., Yang, Y., Song, Y., Liu, J., et al. (2019). Spatial distributions and temporal variations of the near-surface soil freeze state across China under climate change. *Glob. Planet. Change* 172, 150–158. doi:10.1016/j.gloplacha.2018.09.016
- Watanabe, K., and Flury, M. (2008). Capillary bundle model of hydraulic conductivity for frozen soil: Capillary Bundle Model for Frozen Soil: Capillary

bundle model for frozen soil. *Water Resour. Res.* 44, 1–9. doi:10.1029/2008WR007012

Watanabe, K., and Osada, Y. (2016). Comparison of hydraulic conductivity in frozen saturated and unfrozen unsaturated soils. *Vadose Zone J.* 15, 1–7. doi:10.2136/vzj2015.11.0154

Wu, K., Chen, Z., Li, J., Li, X., Xu, J., and Dong, X. (2017). Wettability effect on nanoconfined water flow. *Proc. Natl. Acad. Sci. U.S.A.* 114, 3358–3363. doi:10.1073/pnas.1612608114

Xiao, B., Tu, X., Ren, W., and Wang, Z. (2015). Modeling for hydraulic permeability and kozeny-carman constant of porous nanofibers using A fractal approach. *Fractals* 23 (3), 1550029. doi:10.1142/S0218348X15500292

Xiao, Z., Lai, Y., and Zhang, M. (2018). Study on the freezing temperature of saline soil. *Acta Geotech.* 13, 195–205. doi:10.1007/s11440-017-0537-1

Xu, J., Lan, W., Ren, C., Zhou, X., Wang, S., and Yuan, J. (2021). Modeling of coupled transfer of water, heat and solute in saline loess considering sodium sulfate

crystallization. *Cold Regions Sci. Technol.* 13, 103335. doi:10.1016/j.coldregions.2021.103335

Zhang, X., Wu, Y., Zhai, E., and Ye, P. (2021a). Coupling analysis of the heat-water dynamics and frozen depth in a seasonally frozen zone. *J. Hydrology* 593, 125603. doi:10.1016/j.jhydrol.2020.125603

Zhang, X., Zhai, E., Wu, Y., Sun, D., and Lu, Y. (2021b). Theoretical and numerical analyses on hydro-thermal-salt-mechanical interaction of unsaturated salinized soil subjected to typical unidirectional freezing process. *Int. J. Geomech.* 21, 04021104. doi:10.1061/(ASCE)GM.1943-5622.0002036

Zhang, Y., Fang, J. H., Liu, J. K., Xu, A. H., Traffictransportation, S. O., University, L. J., et al. (2015). Research on the distribution of saline soil along the Chaerhan-Golmud Highway, northwestern China. *Sci. Cold Arid Regions* 7, 189–193. doi:10.3724/SP.J.1226.2015.00189

Zhao, J., and Luo, H. (2019). Transport and crystallization of NaCl solution in porous silicate materials. *J. Cryst. Growth* 519, 25–34. doi:10.1016/j.jcrysgro.2019.05.003